nature human behaviour

Article

https://doi.org/10.1038/s41562-024-01984-8

Human olfactory perception embeds fine temporal resolution within a single sniff

Received: 13 August 2023

Accepted: 13 August 2024

Published online: 14 October 2024

Check for updates

Yuli Wu[1,2], Kepu Chen[1], Chen Xing[1,2], Meihe Huang[1,2], Kai Zhao[3] & Wen Zhou[1,2,4]

A sniff in humans typically lasts one to three seconds and is commonly considered to produce a long-exposure shot of the chemical environment that sets the temporal limit of olfactory perception. To break this limit, we devised a sniff-triggered apparatus that controls odorant deliveries within a sniff with a precision of 18 milliseconds. Using this apparatus, we show through rigorous psychophysical testing of 229 participants (649 sessions) that two odorants presented in one order and its reverse become perceptually discriminable when the stimulus onset asynchrony is merely 60 milliseconds (Cohen's $d = 0.48$; 95% confidence interval, (55, 59); 120-millisecond difference). Discrimination performance improves with the length of stimulus onset asynchrony and is independent of explicit knowledge of the temporal order of odorants or the relative amount of odorant molecules accumulated in a sniff. Our findings demonstrate that human olfactory perception is sensitive to chemical dynamics within a single sniff and provide behavioural evidence for a temporal code of odour identity.

Immersed in a complex and dynamic chemical environment, the human olfactory apparatus nonetheless appears to have a coarse temporal resolution far inferior to that of vision or audition—known to operate on the scale of tens of milliseconds[1]. Humans reportedly cannot discriminate between two odours presented in one order and in the reverse order when the inter-odour interval is as long as 0.6 seconds[2]. Additionally, each olfactory sampling, or sniff, typically takes one to three seconds in humans, and sniffs are separated in time, seconds apart from one another. Human olfaction is thus regarded as in a constant state of change-blindness[3].

However, electrophysiological examinations of odour-induced responses in rodents have long revealed prominent coupling between neural dynamics in the olfactory pathway and rhythmic odour sampling (4–12 Hz)[4]. Rather than an instantaneous bout of bursts, odour responses among mitral/tufted cells (the output neurons of the olfactory bulb) tile the duration of the sniff cycle with precise response timing[5,6] and convey information to downstream olfactory regions at subsniff timescales[7,8]. Such temporal codes have been proposed to represent odour identity or concentration or to aid difficult discriminations of similar odours[8–12]. Moreover, optogenetic studies show that mice are sensitive to the sniff-referenced timing of optogenetically driven activations of olfactory sensory neurons and of a single olfactory glomerulus[13,14] and to the sequence of the spatial patterns of activation of the olfactory bulb[15]. Although it is unclear to what extent optogenetic manipulations resemble odour-evoked responses or produce genuine olfactory experience, these findings suggest that subsniff temporal dynamics in the mammalian olfactory system are behaviourally relevant and lead us to ask whether and in what way they play a role in human olfactory perception.

A major obstacle in assessing subsniff temporal modulation of odour perception in mammals, humans included, is how to present odorants at different phases within a sniff[4]. We have devised an apparatus that overcomes this obstacle and ensures temporal locking of odorant deliveries to sniff onset. This has enabled us to empirically measure human olfactory perceptual sensitivity to subsniff temporal information with a precision on the order of tens of milliseconds.

[1]State Key Laboratory of Brain and Cognitive Science, Institute of Psychology, Chinese Academy of Sciences, Beijing, China. [2]Department of Psychology, University of Chinese Academy of Sciences, Beijing, China. [3]Department of Otolaryngology, Ohio State University, Columbus, OH, USA. [4]Chinese Institute for Brain Research, Beijing, China. e-mail: zhouw@psych.ac.cn

https://doi.org/10.1038/s41562-024-01984-8

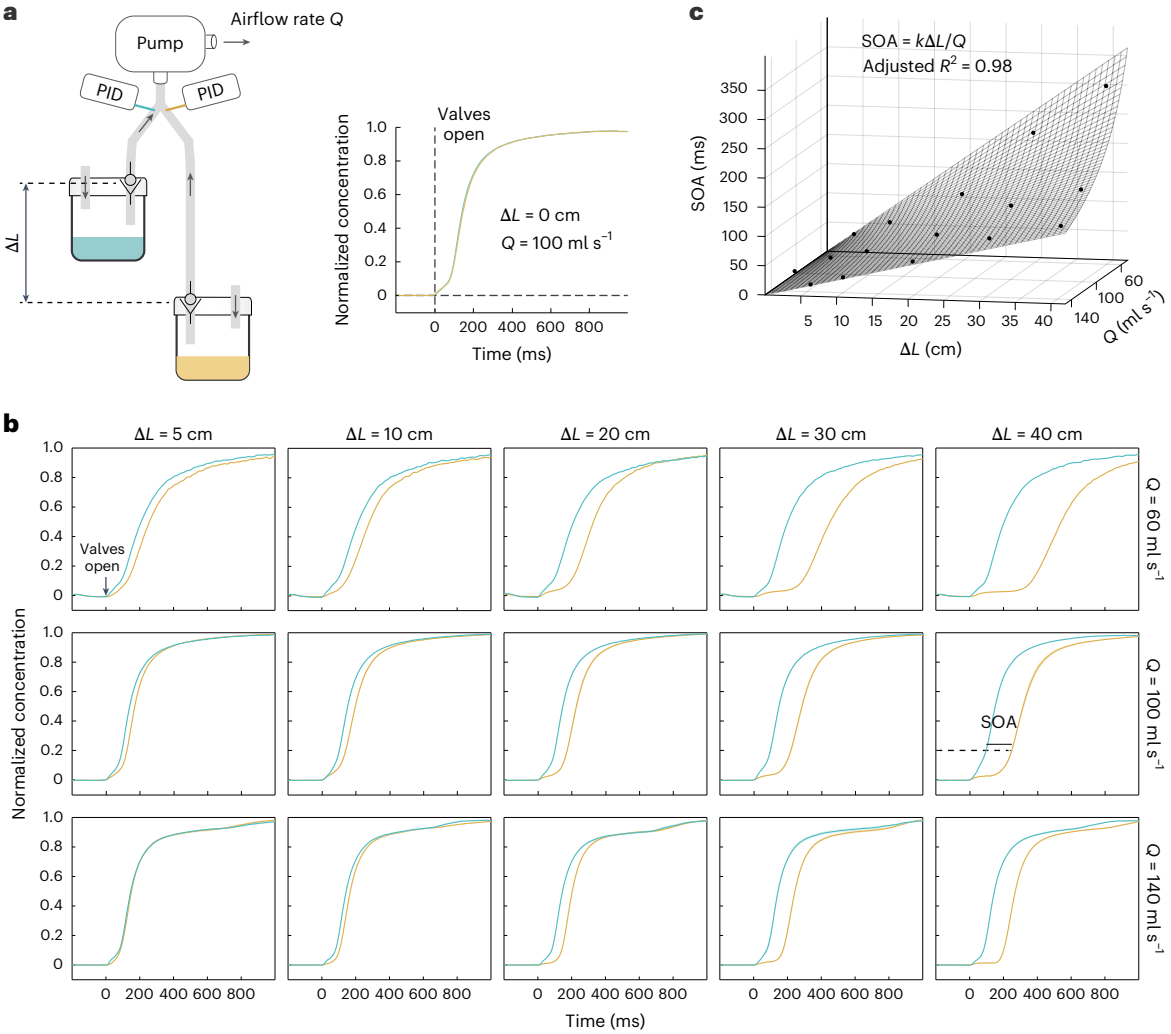

Fig. 1 | Apparatus set-up and measurement of odour SOA. a, The apparatus comprised two check-valve-controlled odour channels with a length difference of Δ*L*, here connected to a miniature vacuum pump. Vapour-phase odour concentrations in the two channels were measured by two calibrated miniature PIDs and showed nearly identical curves over time when Δ*L* = 0. **b**, Time-concentration curves for the two channels under various values of Δ*L* and *Q*. SOA was calculated as the interval between the time points where readings of the two PIDs reached 20% of their respective maxima in a trial. Each subplot represents the average of 32 trials. See also Supplementary Fig. 2a. **c**, The mean SOAs under each combination of Δ*L* and *Q* can be accurately fitted by SOA = $k\Delta L/Q$ (the cross-hatched area). The shaded areas around the curves in **a** and **b** indicate the s.e.m.

Results

Apparatus set-up and control of odour onset asynchrony within a sniff

A sniff is produced by the contraction of the diaphragm, which increases the volume of the thoracic cavity and creates negative pressure that draws air through the nose. The sniff nasal inspiratory pressure ranges from 1 kPa to 14 kPa (ref. 16). We reasoned that this could be exploited to activate valve-gated odour channels. The time taken for odour molecules to reach the nose would then vary with flow rate and the distance between the valve of that channel and the nose (given a channel with a fixed cross-sectional area). The former is directly linked to the amount of negative pressure (sniff vigour) and can be measured; the latter can be experimentally manipulated by adjusting tubing length.

As proof of principle, we devised an apparatus (Fig. 1a, left) that comprised a miniature vacuum pump connected to two Teflon tubes (inside diameter, 3/16″ (4.76 mm)) via a Y structure. One tube was 10 cm long, and the other was 10 + Δ*L* cm. Their other ends were each fitted with a one-way valve (breaking pressure, 1.24 kPa; closing pressure, 0.10 kPa) and a push-to-connect tube fitting that allowed for easy connection and disconnection to an odour bottle containing 10 ml of a 1% v/v isoamyl acetate (tracer) in propylene glycol solution. The inlet needles of two calibrated miniature photo-ionization detectors (PIDs) were inserted in the two tubes close to the Y junction to measure vapour-phase odour concentrations. The tracer molecules in the connected odour bottles could not move into the tubes unless the two check valves were simultaneously opened by negative pressure (pump on), in which case the PIDs would register the latencies of odour arrival and the odour stimulus onset asynchrony (SOA) in between. After each measurement, the odour bottles were detached, and the pump was left on for a few more seconds to remove residual tracer molecules in the tubes (Supplementary Fig. 1). We verified that the apparatus had little systematic error in measurement: measured SOAs were around 0 when Δ*L* = 0 (32 trials; mean, 4 ms; $t_{31} = 0.93$; $P = 0.36$; Cohen's $d = 0.16$; 95% confidence interval (CI), (−4.5, 11.9) ms; Fig. 1a, right). Further assessments under different values of Δ*L* (5, 10, 20, 30 or 40 cm) and the pump's flow rate *Q* (set at 60, 100 or 140 ml s^{-1}) across 480 trials (32 trials per combination; Fig. 1b and Supplementary Fig. 2a) showed that rise time in the 10 cm tube reduced slightly with *Q* (mean, 135, 111 and 100 ms for *Q* = 60, 100 and 140 ml s^{-1}, respectively) and generally fell around 115 ms. Critically, SOA increased with Δ*L*, decreased with *Q* and closely followed a linear relationship with the quotient of Δ*L* and

https://doi.org/10.1038/s41562-024-01984-8

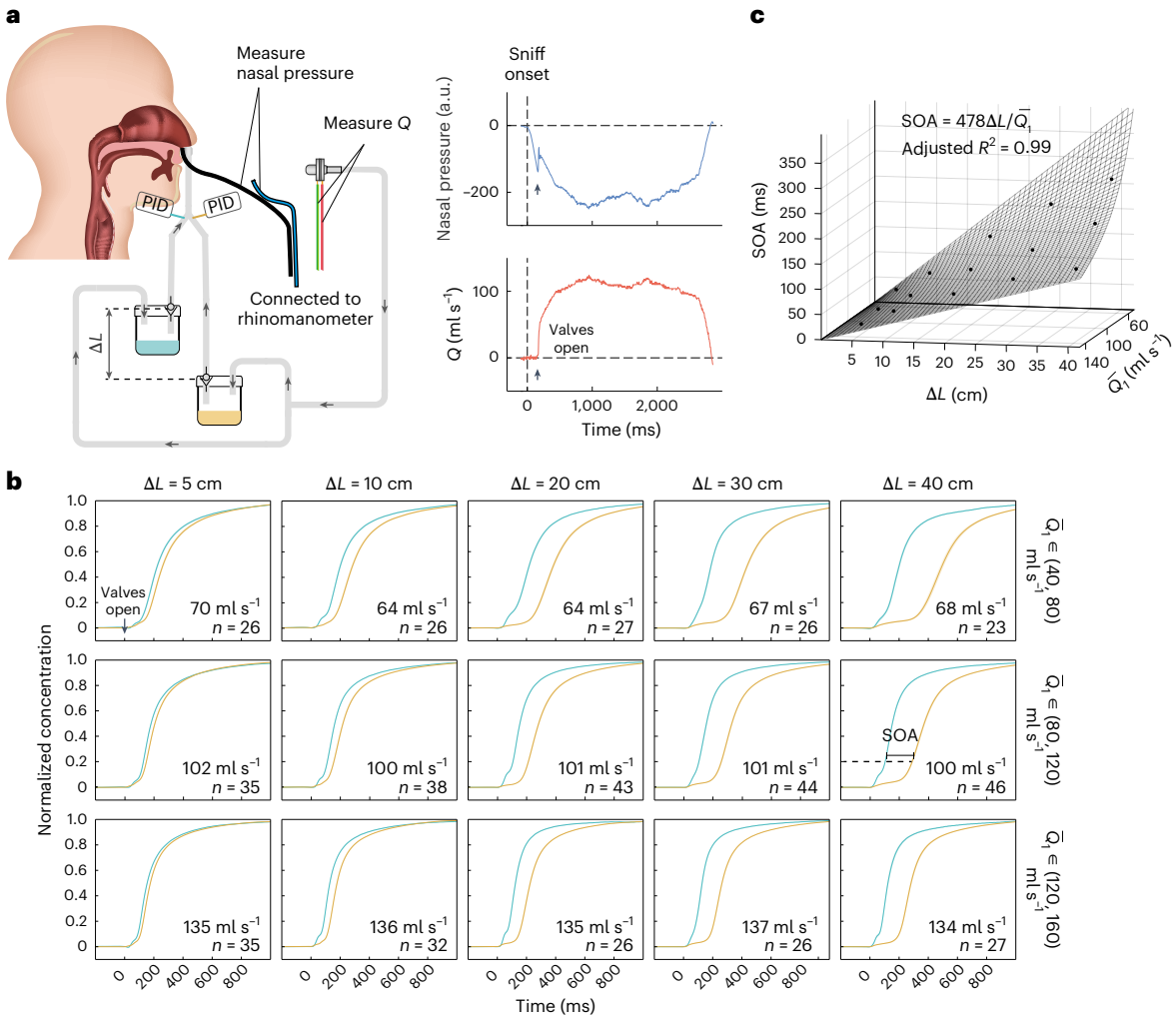

Fig. 2 | Control of odour onset asynchrony within a sniff. a, The apparatus was connected to a Teflon nosepiece for odour sampling. Nasal pressure operated the check valves and controlled the flow rate, which generally peaked within 1 s of sniff onset. Adapted from ref. 50, Royal Society. **b**, Time-concentration curves for the two channels under various values of ΔL and $\bar{Q}_1$. Each subplot represents the average of 23–46 trials. See also Supplementary Fig. 2b. **c**, The mean SOAs in **b** can be accurately fitted by SOA $= 478\Delta L/\bar{Q}_1$ (the cross-hatched area). The shaded areas in **b** indicate the s.e.m.

Q (adjusted $R^2 = 0.98$; Fig. 1c). These observations demonstrate the feasibility of accurately controlling the timing of odorants in a manner that is time-locked to the onset of negative pressure.

Next, we removed the pump and fitted the Y structure with a Teflon nosepiece. For human sniffing experiments, the nosepiece was placed in one nostril, and the other nostril was pinched shut to circumvent potential confounds due to resistance and airflow differences between the two nasal cavities[17]. Residual odour molecules in the tubes were cleared using an air blower (with the odour bottles detached) after each sampling. As illustrated in Fig. 2a, the act of sniffing created negative pressure that opened the check valves and drew air through the odour bottles into the unoccluded nostril, like turning on the vacuum pump. Unlike the pump, though, the flow rates produced by sniffing tended to rise more gradually and could not be set at a fixed value (Supplementary Fig. 3). We measured SOAs and values of Q under various levels of sniff vigour and ΔL values (5, 10, 20, 30 or 40 cm) in 480 trials (Fig. 2b and Supplementary Fig. 2b). The results revealed that SOA could be precisely predicted by ΔL and the average flow rate recorded over the first 1 s of sniffing ($\bar{Q}_1$): SOA $= 478\Delta L/\bar{Q}_1$ (adjusted $R^2 = 0.99$; Fig. 2c). Across all trials, where $\bar{Q}_1$ ranged from 45 to 159 ml s^{-1} (mean ± s.d., 102.1 ± 28.1 ml s^{-1}), the mean absolute residual—the absolute difference between the observed and predicted values of SOA—was 18 ms (interquartile range (IQR), 19 ms (6–25 ms); 95th percentile, 49 ms).

The difference in length between the two tubes resulted in a subtle difference in odorant concentration slopes, potentially due to Taylor dispersion[18]. As shown in Figs. 1b and 2b, the rising portion of the time-concentration curve for the longer tube was slightly less steep than that for the shorter tube when $\Delta L = 40$ cm and Q or $\bar{Q}_1 < 80$ ml s^{-1}. This effect was generally negligible with smaller ΔL values (for example, 10 cm).

Subsniff temporal information modulates odour perception

The apparatus described above enabled us to construct a temporal mixture of two odorants, one preceding the other by a controllable amount of time within a single sniff, and to test whether their order would significantly impact olfactory perception. We used pentyl valerate (PV), an aliphatic ester with an apple-like smell, and isobutyl phenylacetate (IP), an aromatic ester with a sweet floral smell. They are different in structure and smell but have similar diffusivity in air and are easily soluble in mucus (Supplementary Table 1). The odours were comparable in intensity ($t_{29} = -0.15$; $P = 0.88$; Cohen's $d = 0.027$; 95% CI of difference, (−0.4, 0.5)), valence ($t_{29} = 1.25$; $P = 0.22$; Cohen's $d = 0.23$; 95% CI of difference, (−1.0, 0.2)) and nasal pungency (trigeminality; $t_{29} = 0.87$; $P = 0.39$; Cohen's $d = 0.16$; 95% CI of difference, (−0.1, 0.1)) on the basis of odour ratings and lateralization performances[19] by two separate panels of 30 participants each (Supplementary Fig. 4).

https://doi.org/10.1038/s41562-024-01984-8

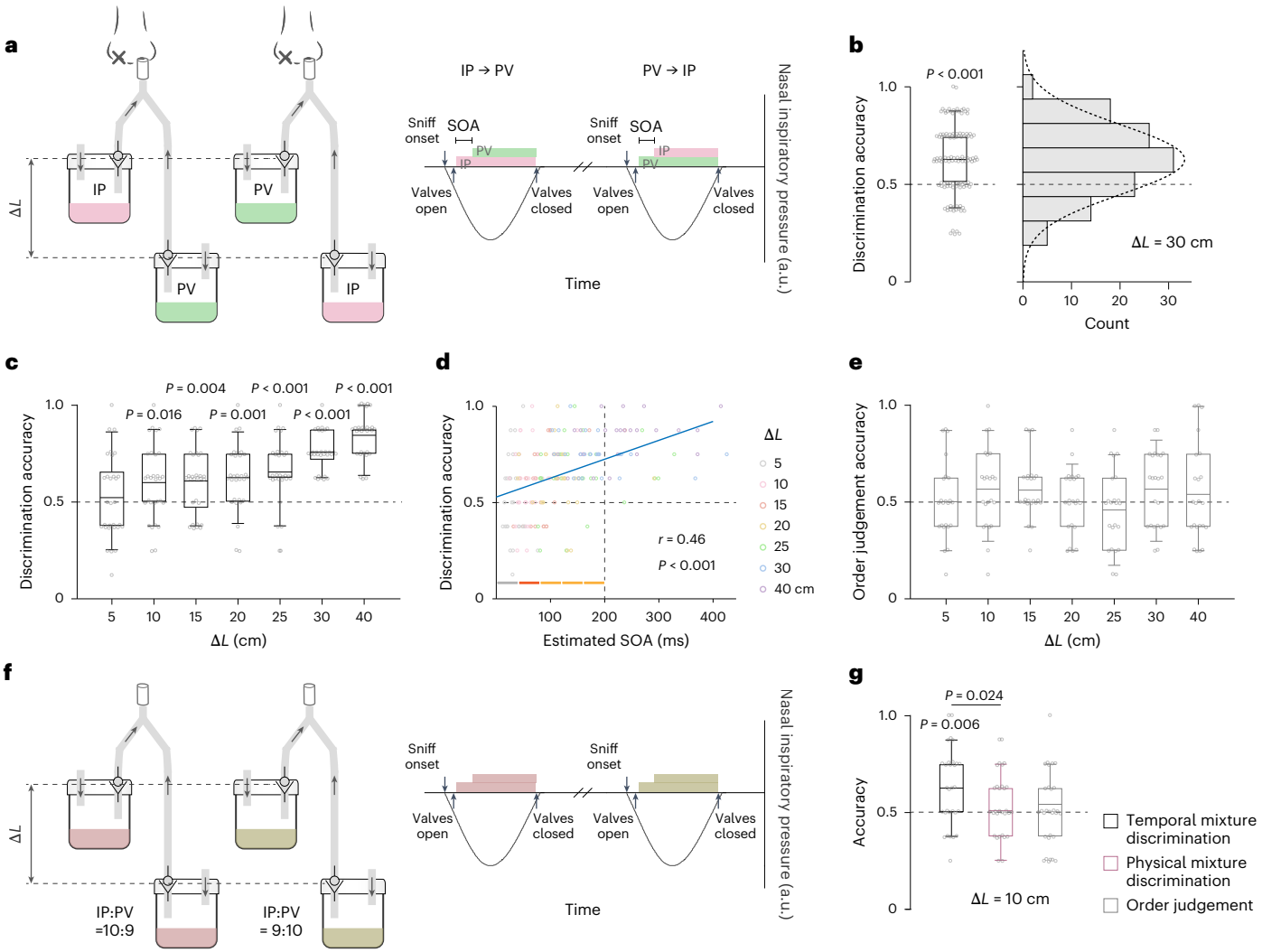

Fig. 3 | Effect of subsniff temporal information on olfactory perception, as tested with PV and IP. a, Schematic illustration of a trial in the temporal mixture discrimination task of PV → IP and IP → PV. Nose drawing adapted from ref. 53, Springer Nature Limited. **b**, Temporal mixture discrimination accuracy and its histogram distribution in Experiment 1 (n = 119 participants) at ΔL = 30 cm (t_{118} = 7.78; $P = 3.07 \times 10^{-12}$; Cohen's d = 0.71; 95% CI, (0.59, 0.66), compared with chance). **c**–**e**, In Experiment 2, temporal mixture discrimination accuracy (n = 30 participants) was significantly above chance for ΔL = 10, 15, 20, 25, 30 and 40 cm (t_{29} = 2.85, 3.56, 4.09, 4.80, 14.42 and 16.88; $P_{cor} = 0.016, 0.004, 1.25 \times 10^{-3}$, 2.20×10^{-4}, 5.53×10^{-14} and 1.07×10^{-15}; Cohen's d = 0.52, 0.65, 0.75, 0.88, 2.63 and 3.08; 95% CIs, (0.53, 0.67), (0.55, 0.67), (0.56, 0.69), (0.59, 0.72), (0.72, 0.79) and (0.80, 0.89), respectively) (**c**) and was positively correlated with estimated SOA (r = 0.46, $P = 7.17 \times 10^{-12}$) (**d**), while order judgement accuracy (n = 23 participants) was at chance level (**e**). The colours of the horizontal bars in **d** reflect levels of significance: grey indicates not significant, red indicates $P < 0.05$ and yellow indicates $P < 0.001$. Discrimination accuracies for PV → IP and IP → PV became significantly above chance when the estimated SOAs were 40–80 ms (t_{41} = 2.39; P_{cor} = 0.042; Cohen's d = 0.37; 95% CI, (0.51, 0.63)). **f**, An example trial in the physical mixture discrimination task. **g**, Although significantly above chance in discerning between PV → IP and IP → PV at ΔL = 10 cm (t_{29} = 3.43; P_{cor} = 0.006; Cohen's d = 0.63; 95% CI, (0.55, 0.70)), the participants (n = 30) in Experiment 3 failed to discriminate between 10:9 and 9:10 physical mixtures of PV and IP, with accuracies significantly lower than those for the temporal mixtures (t_{29} = −2.38; P = 0.024; Cohen's d = 0.43; 95% CI of difference, (−0.22, −0.02)). In each box-and-whisker plot, the central line denotes the mean, the bottom and top edges of the box indicate the 25th and 75th percentiles, and the ends of the whiskers represent the 5th and 95th percentiles. The circles represent individual data points. The P values are two-tailed and are Holm–Bonferroni corrected for multiple comparisons, where applicable.

In Experiment 1, we set ΔL at 30 cm, estimated to produce an SOA of roughly 120–180 ms in a moderate sniff ($\bar{Q}_1$, 80–120 ml s^{-1})—the duration of an eye blink[20]—and tested in a large sample of 119 naive participants whether it generated a perceptual difference between PV preceding IP (PV → IP) and IP preceding PV (IP → PV). The discrimination task consisted of eight trials with a chance level of 0.5. In each trial, the participants, blindfolded, sampled two temporal mixtures consecutively (Fig. 3a)—both PV → IP or both IP → PV in four trials, and PV → IP and IP → PV in the other four trials in random order—and reported whether they smelled the same or different. Of the 952 trials completed (8 × 119), 597 trials were correct (binomial test $P = 4.07 \times 10^{-15}$). Discrimination accuracies across the participants were normally distributed with a mean of 0.63 (t_{118} = 7.78; $P = 3.07 \times 10^{-12}$; Cohen's d = 0.71; 95% CI, (0.59, 0.66); Fig. 3b). Forty-six (38.66%) participants showed accuracies ≥0.75, whereas the percentage expected by chance was 14.45% (χ^2_1 = 56.37, $P = 6.00 \times 10^{-14}$, φ = 0.69). These results strongly point to innate perceptual sensitivity to subsniff chemical dynamics.

We wondered about the upper limit of this temporal sensitivity and whether it translates into explicit knowledge of the temporal order of odour components or a difference in overall perceived odour quality (olfactory character), as predicted by the Hopfield model, where the relative timing of active mitral cells codes odour identity[21]. To this end, we invited those with discrimination accuracies ≥0.75 at ΔL = 30 cm for a detailed examination of 'olfactory temporal acuity' in Experiment 2.

Thirty of them volunteered. The experiment included seven sessions held on seven separate days, with ΔL set at 40, 30, 25, 20, 15, 10 and 5 cm in Sessions 1 to 7, respectively. In each session, the participants completed the temporal mixture discrimination task and an additional order judgement task. In the order judgement task, they were first familiarized with the respective odours of PV and IP and were subsequently presented with PV → IP in four trials and IP → PV in another four trials in random order and asked to indicate in each trial which odour came first. They were instructed to maintain a regular sniff pattern and were assessed for flow rates between the two tasks with clean air to avoid odour contamination. The average $\bar{Q}_1$ and the ΔL for that session were used to calculate the SOA per session per participant.

Overall, the $\bar{Q}_1$ values exhibited notable interindividual variability but were generally stable across the sessions ($F_{6,168} = 0.76$, $P = 0.60$, $\eta_p^2 = 0.027$; Supplementary Fig. 5a). The grand mean of $\bar{Q}_1$ was 88.7 ml s^{-1}. This produced estimated SOAs of 27, 54, 81, 108, 135, 162 and 216 ms under ΔL = 5, 10, 15, 20, 25, 30 and 40 cm, respectively. The corresponding discrimination accuracies averaged across participants were 0.52, 0.60, 0.61, 0.63, 0.65, 0.76 and 0.85 ($t_{29} = 0.53$, 2.85, 3.56, 4.09, 4.80, 14.42 and 16.88; $P = 0.60$, 0.008, 0.001, 3.13×10^{-4}, 4.40×10^{-5}, 9.22×10^{-15} and 1.53×10^{-16}; $P_{cor} = 0.60$, 0.016, 0.004, 1.25×10^{-3}, 2.20×10^{-4}, 5.53×10^{-14} and 1.07×10^{-15}; Cohen's $d = 0.10$, 0.52, 0.65, 0.75, 0.88, 2.63 and 3.08; 95% CIs, (0.44, 0.60), (0.53, 0.67), (0.55, 0.67), (0.56, 0.69), (0.59, 0.72), (0.72, 0.79) and (0.80, 0.89), respectively; Fig. 3c). That is, discrimination accuracy for the temporal mixtures increased monotonically with ΔL (linear effect: $F_{1,29} = 80.05$, $P = 7.73 \times 10^{-10}$, $\eta_p^2 = 0.73$) and was significantly above chance when ΔL was as small as 10 cm. To account for between-participant and between-session $\bar{Q}_1$ variations, we further analysed the discrimination accuracies and estimated SOAs in individual sessions. There was a robust positive correlation between the two across all sessions and participants ($r = 0.46$, $P = 7.17 \times 10^{-12}$; Fig. 3d) and also within participants (across seven sessions, the median of r was 0.66; Supplementary Fig. 5b). When the estimated SOAs fell within 0–40, 40–80, 80–120, 120–160 and 160–200 ms (horizontal bars in Fig. 3d), the discrimination accuracies were on average 0.53, 0.57, 0.64, 0.66 and 0.75 ($t_{27} = 0.84$, $t_{41} = 2.39$, $t_{38} = 5.04$, $t_{30} = 4.94$ and $t_{25} = 10.01$; $P = 0.41$, 0.021, 1.18×10^{-5}, 2.79×10^{-5} and 3.15×10^{-10}; $P_{cor} = 0.41$, 0.042, 4.72×10^{-5}, 8.37×10^{-5} and 1.58×10^{-9}; Cohen's $d = 0.16$, 0.37, 0.81, 0.89 and 1.96; 95% CIs, (0.45, 0.61), (0.51, 0.63), (0.59, 0.70), (0.60, 0.73) and (0.70, 0.81), respectively). Namely, the temporal mixtures of PV → IP and IP → PV became perceptually discriminable when the SOA was merely 40–80 ms (mean, 58 ms; 95% CI, (54, 62) ms).

In contrast, the participants appeared unable to reliably judge the order of PV and IP ($t_{22} = 0.13$, 1.62, 2.02, 0.16, −0.89, 1.74 and 0.84; $P = 0.90$, 0.12, 0.06, 0.88, 0.38, 0.10 and 0.41; Cohen's $d = 0.03$, 0.34, 0.42, 0.03, 0.19, 0.36 and 0.18; 95% CIs, (0.42, 0.59), (0.48, 0.66), (0.50, 0.63), (0.43, 0.58), (0.37, 0.55), (0.49, 0.66) and (0.44, 0.65); for ΔL = 5, 10, 15, 20, 25, 30 and 40 cm, respectively; Fig. 3e). Several of them spontaneously reported smelling a holistic odour that more resembled PV than IP or the other way around but not two sequential odours within a sniff. A closer inspection of the discrimination and order judgement performances revealed that higher discrimination accuracies were associated with idiosyncratic biases in assigning either the former or the latter of a temporal mixture as the one that came first ($r = 0.21$, $P = 0.009$), which corroborated the self-reports and indicates different weights of the former and latter odorants in shaping the perceptual outcome. These findings hence lend support to the Hopfield model[21] and a related "primacy coding" scheme[22], which proposes that the earliest activated receptors form a code for odour identity.

We also considered an alternative possibility. The temporal dynamics of chemical input within a sniff end with that sniff when no more airborne molecules are drawn into the nose. In our case, this results in a higher proportion of PV and a lower proportion of IP in PV → IP than in IP → PV and vice versa (Fig. 3a), which might be the basis for olfactory discrimination. Given a short 1 s sniff with an SOA of 100 ms, the relative proportions of PV and IP in PV → IP and IP → PV were estimated to be roughly 10:9 and 9:10 (ignoring rise time), respectively. The shorter the SOA and the longer the sniff duration, the smaller the proportional difference between the two temporal mixtures. To clarify whether it was the relative proportion of odour molecules that influenced perception, we conducted Experiment 3 and again recruited from the original sample of 119 participants 30 individuals with discrimination accuracies ≥0.75 at ΔL = 30 cm. They were each tested in two sessions held on two consecutive days, where they completed the discrimination and order judgement tasks with PV → IP and IP → PV on one day and another discrimination task with physical mixtures of PV and IP in the proportions of 10:9 and 9:10 on the other day in balanced order. ΔL was set at 10 cm, and the two discrimination tasks were the same in format (Fig. 3a,f). Consistent with earlier results, the participants—while lacking explicit knowledge of the order of IP and PV ($t_{29} = 1.38$; $P = 0.18$; Cohen's $d = 0.25$; 95% CI, (0.48, 0.60))—were well above chance in discerning between PV → IP and IP → PV (mean accuracy, 0.63; $t_{29} = 3.43$; $P = 0.002$; $P_{cor} = 0.006$; Cohen's $d = 0.63$; 95% CI, (0.55, 0.70)). The estimated SOAs were 59 ms on average (IQR across participants, 28 ms). All sniffed longer than 1 s. Nevertheless, their discrimination accuracies for the 10:9 and 9:10 physical mixtures of PV and IP were not different from chance ($t_{29} = 0.24$; $P = 0.81$; Cohen's $d = 0.19$; 95% CI, (0.44, 0.58)) and significantly lower than those for the temporal mixtures ($t_{29} = -2.38$; $P = 0.024$; Cohen's $d = 0.43$; 95% CI of difference, (−0.22, −0.02)) (Fig. 3g).

It remained plausible that physical mixing differed from the vapour mixing of PV and IP. To evaluate this, we examined the relationships between vapour-phase and liquid-phase concentrations for PV and IP (Supplementary Information and Supplementary Fig. 6). On the basis of these assessments, we adjusted the headspace concentrations of PV and IP, each contained in a separate bottle, to achieve specific vapour concentration ratios. We then conducted a preregistered supplementary experiment (https://doi.org/10.17605/OSF.IO/7WTEU), using our apparatus to deliver the vapour mixtures of PV and IP in varying ratios with zero SOA (Supplementary Fig. 7a). Participants in this supplementary experiment were screened, all demonstrating discrimination accuracies ≥0.75 between PV → IP and IP → PV at ΔL = 30 cm. We found that they could not distinguish between the vapour mixtures of PV and IP in 10:9 and 9:10 ratios. However, when subjected to the temporal mixture discrimination task of PV → IP and IP → PV at ΔL = 10 cm, the participants again performed significantly above chance. Their discrimination accuracies were significantly higher than those for the vapour mixtures of PV and IP in 10:9 and 9:10 ratios and, by estimation, roughly corresponded to what would be expected for 10:6 and 6:10 PV:IP vapour mixtures (Supplementary Information and Supplementary Figs. 7 and 8). We therefore concluded that fine temporal information within a sniff modulated perceived odour quality, irrespective of the relative proportions of chemical compounds accumulated in that sniff.

Generalizability test with real-time flow rate measurement

To verify whether the observed fine temporal sensitivity of human olfactory perception extends to other odorants, we introduced two new compounds: citral (CTL), an acyclic monoterpene aldehyde with a fresh lemon-like smell, and dimethyl trisulfide (DMTS), a trisulfide with a sulfurous onion-like smell. These compounds were used as stimuli in a previous study, which found no significant contribution of temporal information to human olfactory perception[2]. They are roughly comparable in diffusivity in air but very different in structure, smell and solubility in mucus, with DMTS being substantially less soluble than CTL (Supplementary Table 1). On the basis of odour ratings and lateralization performances[19] by an independent panel of 30 participants, CTL was significantly more pleasant and numerically but not statistically more pungent than DMTS ($t_{29} = 11.89$ and 1.76; $P = 1.13 \times 10^{-12}$ and 0.090; Cohen's $d = 2.17$ and 0.32; 95% CIs of difference, (2.5, 3.6) and (−0.0, 0.2),

https://doi.org/10.1038/s41562-024-01984-8

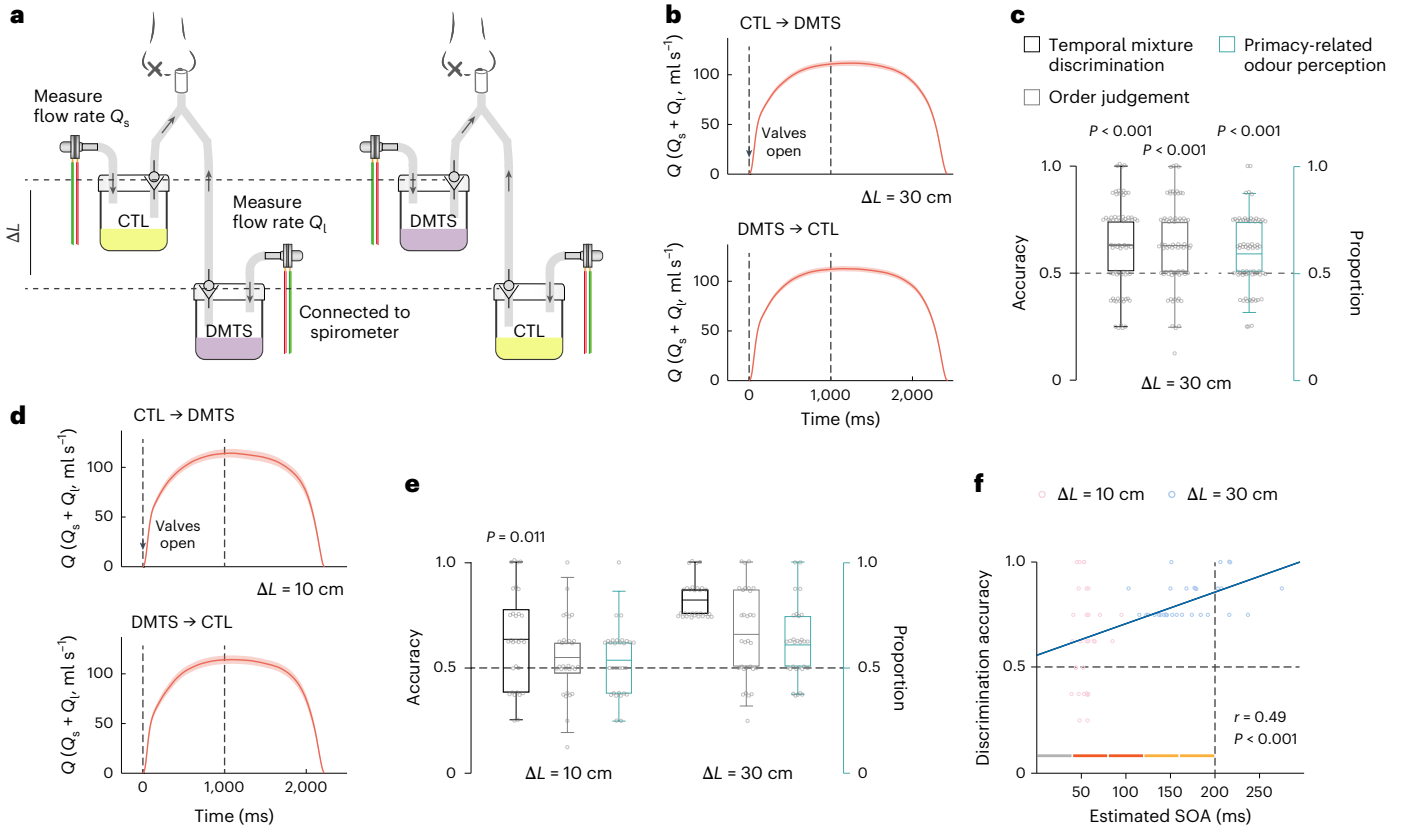

Fig. 4 | Effect of subsniff temporal information on olfactory perception, as tested with CTL and DMTS. a, Schematic illustration of a trial in the temporal mixture discrimination task of CTL → DMTS and DMTS → CTL. Each odour bottle had a separate respiratory flow head connected to its inlet port for real-time measurement of inspiratory flow rates. Flow head adapted from ref. 50, Royal Society; nose drawing adapted from ref. 53, Springer Nature Limited. **b**, Averaged sniff traces across participants in the temporal mixture discrimination task of Experiment 4, at ΔL = 30 cm. **c**, In Experiment 4, at ΔL = 30 cm, the participants (n = 70) were significantly above chance in discriminating between CTL → DMTS and DMTS → CTL and in judging the order of CTL and DMTS (t_{69} = 5.28 and 5.61; P_{cor} = 2.86 × 10^{-6} and 1.19 × 10^{-6}; Cohen's d = 0.63 and 0.67; 95% CIs, (0.58, 0.68) and (0.59, 0.68)). They more frequently reported that the temporal mixture smelled more like its early rather than late component (t_{69} = 4.53; P_{cor} = 2.33 × 10^{-5}; Cohen's d = 0.54; 95% CI, (55.2%, 63.4%)). **d**, Average sniff traces in the temporal mixture discrimination task of Experiment 5, at ΔL = 10 cm. **e**, In Experiment 5, at ΔL = 10 cm, the participants (n = 30) significantly discriminated between CTL → DMTS and DMTS → CTL (t_{29} = 3.18; P_{cor} = 0.011; Cohen's d = 0.58; 95% CI, (0.55, 0.72)). However, their order judgement performances were not different from chance. The reported olfactory percepts were also not significantly biased towards the early or late component of the temporal mixtures. The values from the same participants in Experiment 4 at ΔL = 30 cm are shown for comparison. **f**, Temporal mixture discrimination accuracy was positively correlated with estimated SOA across experiments and participants (r = 0.49, P = 6.55 × 10^{-5}). The horizontal bars are as in Fig. 3d. CTL → DMTS and DMTS → CTL became significantly discriminable (t_{25} = 2.95; P_{cor} = 0.020; Cohen's d = 0.58; 95% CI, (0.54, 0.74)) when the estimated SOAs were 40–80 ms. The sniff traces in **b** and **d** were scaled to the mean sniff duration for each condition. Q_s is the flow rate through the shorter tube; Q_l is the flow rate through the longer tube. The shaded areas indicate the s.e.m. The box-and-whisker plots are as in Fig. 3. The circles represent individual data points. The P values are two-tailed and are Holm–Bonferroni corrected for multiple comparisons, where applicable.

respectively) when the two were matched for olfactory intensity (t_{29} = −1.27; P = 0.21; Cohen's d = 0.21; 95% CI of difference, (−0.8, 0.2)) (Supplementary Fig. 9a,b). As a pair, CTL and DMTS were overall more familiar than the pair PV and IP; CTL and DMTS were also perceptually more distinct from each other than were PV and IP (t_{29} = 2.07 and −7.86; P = 0.047 and 1.16 × 10^{-8}; Cohen's d = 0.38 and 1.43; 95% CIs of difference, (0.0, 1.0) and (−3.0, −1.8), respectively; Supplementary Fig. 9c). Among the four odorants, CTL had the highest familiarity (all $P_{cor} \leq 0.005$). Moreover, we made an important upgrade to our apparatus by connecting a separate respiratory flow head/spirometer to the inlet port of each odour bottle (Fig. 4a). The spirometers were connected to the same data acquisition unit (PowerLab, ADInstruments), and flow rate measurements were synchronized. This enabled real-time measurement of inspiratory flow rates as participants sampled through the apparatus, while also eliminating odour contamination (Supplementary Fig. 10). In doing so, it enhanced our ability to accurately calculate SOAs and improved our assessment of the relationship between SOAs and discrimination performances for temporal odour mixtures.

In Experiment 4, we set ΔL at 30 cm and examined whether it produced a perceptual difference between CTL → DMTS and DMTS → CTL in 70 naive participants. They performed the temporal mixture discrimination task followed by the order judgement task. In each trial of the order judgement task, after sampling either CTL → DMTS or DMTS → CTL, they were asked two questions: which of CTL and DMTS came first and which was more similar to the perceived odour. Their sniff patterns showed no difference between the two tasks ($\bar{Q}_1$: t_{69} = −0.11; P = 0.91; Cohen's d = 0.01; 95% CI of difference, (−2.9, 2.6) ml s^{-1}). On the basis of $\bar{Q}_1$ values recorded per sampling per participant (Supplementary Fig. 11a), we estimated that the SOAs were 167 ms on average with an IQR of 53 ms across all samplings and participants (Supplementary Fig. 11b). The sniff durations were 2,457 ms on average with an IQR of 1,088 ms (Supplementary Fig. 11c). Whereas CTL → DMTS and DMTS → CTL were sampled in the same manner (t_{69} = −1.24 and 0.67; P = 0.22 and 0.51; Cohen's d = 0.15 and 0.08; 95% CIs of difference, (−3.5, 0.8) ml s^{-1} and (−38, 77) ms, for $\bar{Q}_1$ and sniff duration, respectively; Fig. 4b), the participants were

significantly above chance in discriminating between them. Of the 560 (8 × 70) temporal mixture discrimination trials, 354 trials were correct (binomial test $P = 4.17 \times 10^{-10}$). The mean discrimination accuracy across participants was 0.63 (chance = 0.5) ($t_{69} = 5.28$; $P = 1.43 \times 10^{-6}$; $P_{cor} = 2.86 \times 10^{-6}$; Cohen's $d = 0.63$; 95% CI, (0.58, 0.68); Fig. 4c). Thirty-three (47.14%) participants showed accuracies ≥0.75, significantly over the percentage expected by chance (14.45%) ($\chi^2_1 = 60.68$, $P = 6.73 \times 10^{-15}$, $\varphi = 0.93$). These results fully replicated the findings of Experiment 1. Unlike in Experiment 2, though, the participants also exhibited an overall above-chance accuracy of 0.63 in judging the order of CTL and DMTS ($t_{69} = 5.61$; $P = 3.96 \times 10^{-7}$; $P_{cor} = 1.19 \times 10^{-6}$; Cohen's $d = 0.67$; 95% CI, (0.59, 0.68); Fig. 4c). They reported in 59.3% of the cases that the perceived odour was more similar to the early component of the temporal mixture ($t_{69} = 4.53$; $P = 2.33 \times 10^{-5}$; $P_{cor} = 2.33 \times 10^{-5}$; Cohen's $d = 0.54$; 95% CI, (55.2%, 63.4%); Fig. 4c), as predicted by the "primacy coding" scheme[22] (primacy-related odour percepts). There was a significant positive correlation between order judgement accuracy and the proportion of primacy-related odour percepts across participants ($r = 0.45$, $P = 9.42 \times 10^{-5}$; Supplementary Fig. 11d). We reasoned that the familiarity and perceptual distinctiveness of CTL and DMTS probably facilitated categorizations (more similar to CTL or DMTS) of the olfactory percepts elicited by their temporal mixtures. These overt categorizations could have guided the participants' order judgements. Additionally, the large difference in mucosal sorption rate between CTL and DMTS could have come into play and influenced temporal mixture perception[17,23].

In Experiment 5, we further shortened ΔL to 10 cm and recruited 30 participants with discrimination accuracies ≥0.75 for CTL → DMTS and DMTS → CTL at $\Delta L = 30$ cm. The procedures were otherwise identical to those in Experiment 4. As in Experiment 4, the sniff patterns between the temporal mixture discrimination and the order judgement tasks were comparable ($\bar{Q}_1$: $t_{29} = -0.91$; $P = 0.37$; Cohen's $d = 0.17$; 95% CI of difference, (−4.0, 1.5) ml s^{-1}). The SOAs were estimated to be 53 ms on average with an IQR of 13 ms across all samplings and participants (Supplementary Fig. 11e,f). The average sniff duration was 2,236 ms, and the IQR was 939 ms (Supplementary Fig. 11g). The participants again sampled CTL → DMTS and DMTS → CTL in the same manner ($t_{29} = -0.082$ and -0.53; $P = 0.94$ and 0.60; Cohen's $d = 0.02$ and 0.10; 95% CIs of difference, (−3.2, 3.0) ml s^{-1} and (−93, 54) ms, for $\bar{Q}_1$ and sniff duration, respectively; Fig. 4d) and significantly discriminated between them at $\Delta L = 10$ cm (mean accuracy, 0.63; $t_{29} = 3.18$; $P = 0.0035$; $P_{cor} = 0.011$; Cohen's $d = 0.58$; 95% CI, (0.55, 0.72); Fig. 4e). However, their order judgement performances were not different from chance ($t_{29} = 1.51$; $P = 0.14$; Cohen's $d = 0.28$; 95% CI, (0.48, 0.62); Fig. 4e). The reported olfactory percepts were also not significantly biased towards the early or late component of the temporal mixtures ($t_{29} = 1.27$; $P = 0.21$; Cohen's $d = 0.23$; 95% CI, (0.48, 0.60); Fig. 4e). There remained a significant positive correlation between order judgement accuracy and the proportion of primacy-related odour percepts ($r = 0.43$, $P = 0.018$; Supplementary Fig. 11h), corroborating our earlier inference that the order judgements were based in part on the subjective olfactory similarities between a given temporal mixture and its components. Since the participants took part in both Experiments 4 and 5, we also examined their discrimination accuracies, estimated SOAs and sniff durations per ΔL value per participant. Temporal mixture discrimination accuracy was significantly correlated with estimated SOA ($r = 0.49$, $P = 6.55 \times 10^{-5}$; Fig. 4f) but not sniff duration ($r = 0.10$, $P = 0.44$) across experiments and participants. Critically, CTL → DMTS and DMTS → CTL became significantly discriminable (mean accuracy, 0.64; $t_{25} = 2.95$; $P = 0.0067$; $P_{cor} = 0.020$; Cohen's $d = 0.58$; 95% CI, (0.54, 0.74)) when the estimated SOAs were merely 40–80 ms (mean, 54 ms; 95% CI, (51, 56) ms), just like PV → IP and IP → PV (Figs. 3d and 4f). These observations thus echoed the main findings of Experiments 2 and 3 (Supplementary Table 2).

Discussion

Through the design and development of an apparatus that controls odorant delivery within a sniff with a precision (mean absolute deviation) of 18 ms, we have shown in human adults that a sniff of odours is not a long-exposure shot (sniff duration) of the chemical environment that averages out temporal variations. Instead, it embeds fine temporal information. In two sets of psychophysical experiments involving distinct olfactory stimuli, an onset asynchrony of only ~60 ms consistently produced a disparity between the perceived qualities of two compounds when presented in one order versus the reverse order, and discrimination performances improved with longer SOAs (Supplementary Table 2). This occurred independent of the relative amounts of the two compounds accumulated in a sniff or explicit knowledge of their temporal order. Such temporal sensitivity (~120 ms) is on par with that for colour perception (chromatic critical fusion frequency, 10–20 Hz)[24], thus refuting the widely held belief that olfaction is our slow sense. Meanwhile, these findings provide empirical evidence for the hitherto speculated existence of a temporal code for odour identity[21,22] and could guide the design and development of electronic noses and olfactory virtual-reality systems. It is worth noting that the constituents of the temporal mixtures in the current study are generally dissimilar in both structure and odour quality. Conceivably, resolving the dynamics of compounds that bear a high similarity in structure and quality would be more challenging, due to the intrinsic difficulty of discriminating between them.

High temporal sensitivities to pheromones, plant odours and synthetic compounds have been observed in the insect olfactory system, where odour detection is not constrained by sniffing or respiration[25–27]. Olfactory receptor neurons can resolve fluctuating odour stimuli at frequencies exceeding 100 Hz (ref. 26). Odour-evoked responses in projection neurons exhibit oscillations of 20 to 30 Hz. Downstream Kenyon cells, which have brief but renewed (once per oscillatory cycle) integration windows, appear to function as selective coincidence detectors on periodic input from projection neurons[28]. Despite the sparseness of odour representations in Kenyon cells, their responses are consistent with piecewise temporal decoding of the population output of projection neurons[29]. Furthermore, stimulus-specific variations on the order of tens to hundreds of milliseconds in the timing of Kenyon cell spikes alter the responses of downstream neurons in the mushroom body[27]. The temporal sensitivity observed in human olfactory perception appears comparable to the temporal resolution at higher processing stages of the insect olfactory system. Given the commonalities between the insect and mammalian olfactory systems[30] and considering that the output of the mammalian olfactory bulb contains information about the fine temporal structures of odours[31], we postulate that piriform neurons, which are morphologically analogous to Kenyon cells and characterized by response sparseness, could utilize subsniff temporal dynamics in olfactory input and convert them into a spatiotemporal representation of odour quality[32]. The temporal information carried in spike timing could increase the coding capacity of neurons and facilitate discrimination between different odorants, particularly the segregation of temporally adjacent odorants that arise from spatially separate sources[25,26,33]. It has been demonstrated in mice, rats and sharks, and with controversies in humans, that intervals on the order of a few tens to a hundred milliseconds can be efficiently exploited to localize odour sources[31,34–36]. Ultimately, the temporal precision with which odours are processed forms the cornerstone of our ability to resolve the kinetics of olfactory input and to navigate in a dynamic chemical environment. In contrast, individuals with schizophrenia exhibit a fundamental disturbance in the temporal coordination of perceptual processing[37,38]. They also exhibit substantial deficits in olfactory perception across all domains[39].

The temporal sensitivity observed here is an order of magnitude below that reported previously for human olfaction[2,40]. The discrepancy is probably related to the temporal precision with which odorants

are delivered in reference to sniff onset. Commercially available olfactometers do not allow for sniff-triggered variable-latency odorant delivery. Although participants can be cued to initiate sniffing just prior to the programmed delivery of odours, the timing of the odour encounter inevitably varies from one sniff to the next[2]. In contrast, our approach provides significantly improved precision in stimulus control relative to the onset of inhalation (Supplementary Table 3). Moreover, odorants are presented continuously (naturally sniffed in) in the current study, as opposed to in short pulses as done previously[2]. The large sample size employed here also provides us with sufficient statistical power to detect the effect of very brief odour onset asynchronies that might otherwise be missed (see Supplementary Discussion for detailed analyses).

Other than methodological disparities, the discrepancy may also reflect in part the different temporal limits associated with different aspects of perceptual processing, as has been well documented in vision[41] and audition[42]. Plausibly, the representations of odour quality, valence and temporal changes thereof reside at different levels of a temporal processing hierarchy[2,43,44]. It has been argued that odorants in physical binary mixtures are processed with latency differences on the order of hundreds of milliseconds and recognized in series[23], which forms a temporal structure similar to that of words[45]. 'Faster' odorants, those that more easily pass through mucus, are thought to suppress the perception of 'slower' odorants. In our study, CTL has a much higher mucosal sorption rate than DMTS. Nonetheless, the participants were not biased towards perceiving their temporal mixtures as more CTL-like regardless of ΔL value (all $P > 0.12$). Nor were they more likely to judge CTL as the odorant that came first (all $P > 0.22$). Overall, discrimination between a pair of temporal mixtures is not contingent on accurate recognition of the order of the constituent odorants and seems to be underpinned by a mechanism that operates on a much faster timescale than that involved in the serial recognition of mixture components[29,44].

We note that our apparatus lacks some of the versatility of standard in-line olfactometers[46]. It has little control over stimulus duration or the shape of the odour pulse. However, it capitalizes on the dynamics of natural sniffing rather than discounting them. In combination with measurements and monitoring of inspiratory flow rates, it provides precise and fine temporal control of odorant deliveries that are time-locked to sniff onset. In this light, the current study opens up avenues for research on the temporal properties of olfactory perception.

As we breathe in and out, molecules incessantly waft around in the air and are continuously taken in and expelled out of the two nostrils. The temporal dynamics captured within a sniff and among consecutive sniffs, together with the spatial gradients extracted from binaral inputs[47,48], could interweave to form a spatiotemporal landscape of the chemical environment that we experience as smells, vivid and fleeting.

Methods

The study was conducted in accordance with the ethical standards set forth in the Declaration of Helsinki and received approval from the Institutional Review Board at the Institute of Psychology, Chinese Academy of Sciences (H22015).

Apparatus

As shown in Figs. 1a, 2a, 3a and 4a, the apparatus we devised mainly comprised two valve-gated odour channels connected to either a miniature vacuum pump or a Teflon nosepiece (for olfactory sampling) via a Y structure. The channels were Teflon tubes 3/16″ (4.76 mm) in inner diameter and 10 cm and 10 + ΔL cm in length, respectively, with the other ends each fitted with a nylon miniature check valve (Cole-Parmer, fluorosilicone diaphragm; breaking pressure, 1.24 kPa; closing pressure, 0.10 kPa) and a push-to-connect tube fitting. The tube fittings allowed for easy connection and disconnection to two identical 280 ml glass bottles.

Measurement and control of odour onset asynchrony

The SOAs between the two valve-gated odour channels were measured with two calibrated miniature PIDs (Aurora Scientific), whose inlet needles were inserted into the two tubes close to the Y junction (Figs. 1a and 2a). The inlet flow rate was set to 'low', which corresponded to a sampling rate of 750 SCCM or 12.5 ml s^{-1}. Isoamyl acetate (1% v/v in propylene glycol) was used as the tracer for its low ionization potential[44].

Odour channels connected to the pump. SOAs were first assessed under $\Delta L = 0$ and $Q = 100$ ml s^{-1} (Fig. 1a, right) and then under 15 different combinations of ΔL (5, 10, 20, 30 or 40 cm) and Q values (60, 100 or 140 ml s^{-1}) (Fig. 1b and Supplementary Fig. 2a). There were 32 trials per combination, totalling 512 trials. Each trial comprised the following steps: (1) connect the odour bottles, (2) turn on the vacuum pump, (3) wait for ~2 s for the PIDs to register odour arrival latencies and disconnect the odour bottles, and (4) wait for ~5 s for the vacuum pump to clear residual tracer molecules in the tubes (Supplementary Fig. 1) and turn off the pump. Rise time was operationally defined as the time taken for the odour concentration in a channel to reach 20% of the maximum value. SOA was calculated as the interval between the time points where readings of the two PIDs (baseline normalized; baseline, −200 to −50 ms) reached 20% of their respective maxima in a trial (0 to 1,500 ms), which essentially represented the horizontal distance between the rising portions of the time-concentration curves for the two channels (Fig. 1b). The mean SOAs for each combination of ΔL and Q values were fitted with $\mathrm{SOA} = k\Delta L/Q$ (Fig. 1c). The PID data were recorded using LabChart v.8 (ADInstruments) and analysed with MATLAB v.2018a (MathWorks).

Odour channels connected to the nosepiece. Two of the authors repetitively tested the apparatus on themselves to examine how SOA was influenced by ΔL and sniff pattern. As illustrated in Fig. 2a, nasal pressure and odour flow rate during sniffing were first recorded with a rhinomanometer and its inbuilt software NR6 Clinical 3.2.0.1106 (NR6, GM Instruments) using adapted anterior rhinomanometry[49,50] to confirm that sniffing could be exploited to trigger odour delivery. The apparatus was subsequently connected to a spirometer (ADInstruments) in a set-up like that in Fig. 2a but without the pressure tubes to measure SOAs and flow rates under various levels of sniff vigour and ΔL values (5, 10, 20, 30 or 40 cm) in a total of 480 trials. The PID and flow rate data were recorded with LabChart v.8 and subsequently analysed with MATLAB v.2018a. Each trial consisted of the following steps: (1) connect the odour bottles, (2) place the nosepiece in one nostril and inhale for ~2 s while closing the other nostril (care was taken to avoid moisture in the nasal cavity interfering with the PID recordings by starting sniffing immediately after the nosepiece was in place), (3) disconnect the odour bottles, and (4) clear residual tracer molecules in the tubes with an air blower. Flow rates produced by sniffing generally peaked slowly within 1 s of sniff onset, with slopes determined by sniff strengths (Fig. 2a and Supplementary Fig. 3). Concentrations in the odour channels also plateaued within 1 s (Fig. 2b). The trials were thus grouped by ΔL and the average flow rate registered by the flowmeter (spirometer) over the first 1 s of sniffing ($\bar{Q}_1$) (40–80, 80–120 and 120–160 ml s^{-1}; for trials with sniff duration <1 s, $\bar{Q}_1$ was the average flow rate over the duration of sniff). There were 96 trials per ΔL value and 23–46 trials per combination of ΔL and $\bar{Q}_1$. The mean SOAs and $\bar{Q}_1$ values for each combination were fitted with $\mathrm{SOA} = k\Delta L/\bar{Q}_1$ (Fig. 2c), on the basis of which the absolute residuals across all trials—the absolute differences between the observed and predicted values of SOA—were calculated. We note that the recorded flow rates ($\bar{Q}_1$ values) here comprised two sources: sniffing and the inlet flows of the PIDs. However, the relationship between SOA and the quotient of ΔL and $\bar{Q}_1$ was essentially invariant to variations in the values of ΔL or $\bar{Q}_1$ and oblivious to the specific sources of $\bar{Q}_1$ (Supplementary Information and Supplementary Fig. 12). In other words, this relationship held whether $\bar{Q}_1$ was

driven by a combination of sniffing and PID suction or by sniffing alone (as in subsequent behavioural experiments).

Olfactory stimuli

The olfactory stimuli used in behavioural Experiments 1–3, as well as the supplementary experiment, consisted of PV (2% v/v in propylene glycol, 10 ml), IP (10% v/v in propylene glycol, 10 ml), their 9:10 (0.95% and 5.26% v/v of PV and IP, respectively, in propylene glycol, 10 ml) and 10:9 (1.05% and 4.74% v/v of PV and IP, respectively, in propylene glycol, 10 ml) physical mixtures, and their vapour mixtures in the ratios of 10:9 and 9:10, 10:7 and 7:10, and 10:5 and 5:10 (Supplementary Fig. 6c). Those used in behavioural Experiments 4 and 5 consisted of CTL (4% v/v in propylene glycol, 10 ml) and DMTS (0.01% v/v in propylene glycol, 10 ml). They were contained in identical 280 ml glass bottles and were suprathreshold to all participants. The diffusivity and air/mucus partition coefficient[51] of each compound are listed in Supplementary Table 1.

Participants

A total of 388 healthy non-smokers participated in the behavioural assessments. Among these, 189 took part in the main experiments, 109 were screened for the supplementary experiment and 90 rated the perceptual properties (for example, intensity and pleasantness) of the olfactory stimuli and/or were tested for their nasal pungencies (trigeminality) (Supplementary Information). Of those in the main experiments, 119 (60 females, 23.1 ± 2.6 yr) were assessed for olfactory discrimination between the temporal mixtures of PV → IP and IP → PV at ΔL = 30 cm in Experiment 1. Of these, 46 (25 females, 22.4 ± 2.8 yr) showed accuracies ≥0.75 and were invited for follow-up Experiments 2 and 3. There were 30 participants in each of Experiments 2 and 3 (Experiment 2: 16 females, 23.0 ± 2.3 yr; Experiment 3: 16 females, 22.2 ± 2.2 yr); 14 took part in both follow-ups. Another 70 participants (36 females, 23.5 ± 2.3 yr) were assessed with CTL → DMTS and DMTS → CTL at ΔL = 30 cm in Experiment 4; of those with discrimination accuracies ≥0.75, 30 (18 females, 23.3 ± 1.7 yr) were further tested in Experiment 5 at ΔL = 10 cm. Of those screened for the supplementary experiment, 44 (26 females, 22.7 ± 2.5 yr) showed accuracies ≥0.75 for the temporal mixtures of PV → IP and IP → PV at ΔL = 30 cm. Forty of these participants (23 females, 22.6 ± 2.5 yr) were further tested for the discriminations of the vapour mixtures of PV and IP in varying ratios and of the temporal mixtures of PV → IP and IP → PV at ΔL = 10 cm. All participants self-reported having a normal sense of smell and no respiratory allergy or upper respiratory infection at the time of testing. Written informed consent and consent to publish were obtained from all participants.

Behavioural assessments

Temporal mixture discrimination. Temporal mixtures of PV → IP and IP → PV and those of CTL → DMTS and DMTS → CTL were constructed by connecting the corresponding odour bottles to the described apparatus, one to each odour channel. To shorten the retention interval separating the temporal mixtures to be discriminated[52], we made two sets of the apparatus for each ΔL value used. In each trial, the participants were blindfolded and took one sniff from each of the two sets (Figs. 3a and 4a). They reported whether the two odours smelled the same or different. The participants were instructed to maintain a regular sniff pattern and to sample the odours with a fixed nostril (left or right, balanced across participants) while closing the other nostril. The task consisted of eight trials: the temporal mixtures presented in Experiments 1–3 were both PV → IP or both IP → PV in four trials, and PV → IP and IP → PV in the other four trials, in random order; those presented in Experiments 4 and 5 were both CTL → DMTS or both DMTS → CTL in four trials, and CTL → DMTS and DMTS → CTL in the other four trials, in random order. Prior to formal testing, the participants completed a short practice where they were familiarized with the apparatus and the discrimination task.

Order judgement. The participants in Experiments 2 and 3 were familiarized with the respective odours of PV and IP. Afterwards, they were presented with PV → IP in four trials and IP → PV in another four trials, in random order. They were asked to indicate in each trial which of PV and IP came first. The participants in Experiments 4 and 5 were familiarized with the respective odours of CTL and DMTS. Afterwards, they were presented with CTL → DMTS in four trials and DMTS → CTL in another four trials, in random order. They were asked to indicate in each trial which of CTL and DMTS came first and which was more similar to the perceived odour. They sampled the odours in the same manner as in the temporal mixture discrimination task.

Flow rate measurement. The participants in Experiments 2 and 3 were assessed for sniff-induced flow rates between the temporal mixture discrimination and the order judgement tasks. They took ten sniffs through the apparatus (five sniffs per set), connected to two empty bottles and a spirometer (Supplementary Fig. 3, left), in the same manner as in the olfactory tasks. The recording window was set at 2 s for each sniff. The average $\bar{Q}_1$ over the ten sniffs was calculated for each participant and each session. Due to practical constraints at the time of these two experiments, flow rates were not measured concomitantly during the olfactory tasks to avoid odour contamination. The apparatus was subsequently upgraded to enable real-time measurement of inspiratory flow rates while also eliminating odour contamination (Fig. 4a). In Experiments 4 and 5, flow rates were continuously recorded as the participants sampled through the apparatus.

Physical mixture discrimination. The physical mixture discrimination task in Experiment 3 was identical to the temporal mixture discrimination task other than the olfactory stimuli employed. In each trial, the participants were presented with two binary mixtures of PV and IP and reported whether they smelled the same or different. The PV/IP ratios of the mixtures were both 9:10 or both 10:9 in four trials, and 9:10 and 10:9 in four trials, in random order. The two odour bottles connected to each set of the apparatus contained the same binary mixture; no stimulus asynchrony was involved (Fig. 3f).

General procedure. All 119 participants in Experiment 1 completed the temporal mixture discrimination task at ΔL = 30 cm. In Experiment 2, of the 30 participants, 30 completed the temporal mixture discrimination task and 23 completed the order judgement task in all sessions. Additionally, 29 were assessed for sniff-induced flow rates. ΔL varied across the sessions with values of 40, 30, 25, 20, 15, 10 and 5 cm in Sessions 1 to 7, respectively. In Experiment 3, all 30 participants completed the temporal mixture discrimination, order judgement, flow rate measurement and physical mixture discrimination tasks with ΔL fixed at 10 cm. In Experiments 4 and 5, all participants (70 in Experiment 4 and 30 in Experiment 5) completed the temporal mixture discrimination and order judgement tasks at ΔL = 30 cm and 10 cm, respectively; their inspiratory flow rates were simultaneously recorded as they sampled the temporal mixtures. In all of the olfactory tasks, there was a break of at least 60 s between two trials to eliminate olfactory adaptation. Odour residuals in the apparatus were cleared during intertrial intervals.

Behavioural analysis. Behavioural analyses were performed in SPSS (v.26, IBM). SOAs were estimated as a function of $\bar{Q}_1$ and ΔL: $\mathrm{SOA} = 478\Delta L/\bar{Q}_1$. Responses in the odour lateralization, temporal mixture discrimination, order judgement, and physical mixture or vapour mixture discrimination tasks were compared against chance (0.5) using one-sample *t*-tests. In Experiments 1 and 4, binomial exact tests and chi-squared tests were also performed to characterize temporal mixture discrimination accuracies. In Experiment 2, Pearson's correlation tests were performed to assess whether participants' discrimination accuracies for PV → IP and IP → PV were related to the SOAs and to their

absolute deviations from chance level in judging the temporal orders of PV and IP. In Experiment 3 and the supplementary experiment, paired-samples *t*-tests were conducted to compare the discrimination accuracies for the temporal mixtures with those for the physical mixtures or vapour mixtures of PV and IP. In Experiments 4 and 5, Pearson's correlation tests were performed to assess the relationship between order judgement accuracies and proportions of primacy-related olfactory percepts across participants and to test whether participants' discrimination accuracies for CTL → DMTS and DMTS → CTL were related to the SOAs and sniff durations. The effect size for the *t*-tests was estimated using Cohen's *d*. All statistical tests in Experiments 1–5 were two-tailed, as applicable. Those involving multiple comparisons were corrected using the Holm–Bonferroni procedure. In the preregistered supplementary experiment, one-tailed *t*-tests were employed to compare the discrimination accuracies both against chance and between different conditions, and were not corrected for multiple comparisons.

Reporting summary

Further information on research design is available in the Nature Portfolio Reporting Summary linked to this article.

Data availability

All reported data are available at https://doi.org/10.57760/sciencedb.psych.00224.

Code availability

MATLAB scripts for analysing airflow and PID measurements are available at https://doi.org/10.57760/sciencedb.psych.00224.

References

1. Mauk, M. D. & Buonomano, D. V. The neural basis of temporal processing. *Annu. Rev. Neurosci.* **27**, 307–340 (2004).
2. Perl, O., Nahum, N., Belelovsky, K. & Haddad, R. The contribution of temporal coding to odor coding and odor perception in humans. *eLife* **9**, e49734 (2020).
3. Sela, L. & Sobel, N. Human olfaction: a constant state of change-blindness. *Exp. Brain Res.* **205**, 13–29 (2010).
4. Wachowiak, M. All in a sniff: olfaction as a model for active sensing. *Neuron* **71**, 962–973 (2011).
5. Bathellier, B., Buhl, D. L., Accolla, R. & Carleton, A. Dynamic ensemble odor coding in the mammalian olfactory bulb: sensory information at different timescales. *Neuron* **57**, 586–598 (2008).
6. Shusterman, R., Smear, M. C., Koulakov, A. A. & Rinberg, D. Precise olfactory responses tile the sniff cycle. *Nat. Neurosci.* **14**, 1039–1044 (2011).
7. Haddad, R. et al. Olfactory cortical neurons read out a relative time code in the olfactory bulb. *Nat. Neurosci.* **16**, 949–957 (2013).
8. Cury, K. M. & Uchida, N. Robust odor coding via inhalation-coupled transient activity in the mammalian olfactory bulb. *Neuron* **68**, 570–585 (2010).
9. Spors, H. & Grinvald, A. Spatio-temporal dynamics of odor representations in the mammalian olfactory bulb. *Neuron* **34**, 301–315 (2002).
10. Iwata, R., Kiyonari, H. & Imai, T. Mechanosensory-based phase coding of odor identity in the olfactory bulb. *Neuron* **96**, 1139–1152 e1137 (2017).
11. Junek, S., Kludt, E., Wolf, F. & Schild, D. Olfactory coding with patterns of response latencies. *Neuron* **67**, 872–884 (2010).
12. Schaefer, A. T. & Margrie, T. W. Spatiotemporal representations in the olfactory system. *Trends Neurosci.* **30**, 92–100 (2007).
13. Smear, M., Shusterman, R., O'Connor, R., Bozza, T. & Rinberg, D. Perception of sniff phase in mouse olfaction. *Nature* **479**, 397–400 (2011).
14. Smear, M., Resulaj, A., Zhang, J., Bozza, T. & Rinberg, D. Multiple perceptible signals from a single olfactory glomerulus. *Nat. Neurosci.* **16**, 1687–1691 (2013).
15. Chong, E. et al. Manipulating synthetic optogenetic odors reveals the coding logic of olfactory perception. *Science* **368**, eaba2347 (2020).
16. Heritier, F., Rahm, F., Pasche, P. & Fitting, J. W. Sniff nasal inspiratory pressure: a noninvasive assessment of inspiratory muscle strength. *Am. J. Respir. Crit. Care Med* **150**, 1678–1683 (1994).
17. Sobel, N., Khan, R. M., Saltman, A., Sullivan, E. V. & Gabrieli, J. D. The world smells different to each nostril. *Nature* **402**, 35 (1999).
18. Taylor, G. The dispersion of matter in turbulent flow through a pipe. *Proc. R. Soc. Lond. A* **223**, 446–468 (1954).
19. Wysocki, C. J., Cowart, B. J. & Radil, T. Nasal trigeminal chemosensitivity across the adult life span. *Percept. Psychophys.* **65**, 115–122 (2003).
20. Benedetto, S. et al. Driver workload and eye blink duration. *Transp. Res. F Traffic Psychol. Behav.* **14**, 199–208 (2011).
21. Hopfield, J. J. Pattern recognition computation using action potential timing for stimulus representation. *Nature* **376**, 33–36 (1995).
22. Wilson, C. D., Serrano, G. O., Koulakov, A. A. & Rinberg, D. A primacy code for odor identity. *Nat. Commun.* **8**, 1477 (2017).
23. Laing, D. G., Eddy, A., Francis, G. W. & Stephens, L. Evidence for the temporal processing of odor mixtures in humans. *Brain Res.* **651**, 317–328 (1994).
24. De Lange Dzn, H. Research into the dynamic nature of the human fovea–cortex systems with intermittent and modulated light. II. Phase shift in brightness and delay in color perception. *J. Opt. Soc. Am.* **48**, 784–789 (1958).
25. Baker, T. C., Fadamiro, H. Y. & Cosse, A. A. Moth uses fine tuning for odour resolution. *Nature* **393**, 530 (1998).
26. Szyszka, P., Gerkin, R. C., Galizia, C. G. & Smith, B. H. High-speed odor transduction and pulse tracking by insect olfactory receptor neurons. *Proc. Natl Acad. Sci. USA* **111**, 16925–16930 (2014).
27. Gupta, N. & Stopfer, M. A temporal channel for information in sparse sensory coding. *Curr. Biol.* **24**, 2247–2256 (2014).
28. Perez-Orive, J. et al. Oscillations and sparsening of odor representations in the mushroom body. *Science* **297**, 359–365 (2002).
29. Broome, B. M., Jayaraman, V. & Laurent, G. Encoding and decoding of overlapping odor sequences. *Neuron* **51**, 467–482 (2006).
30. Kay, L. M. & Stopfer, M. Information processing in the olfactory systems of insects and vertebrates. *Semin. Cell Dev. Biol.* **17**, 433–442 (2006).
31. Ackels, T. et al. Fast odour dynamics are encoded in the olfactory system and guide behaviour. *Nature* **593**, 558–563 (2021).
32. Rennaker, R. L., Chen, C. F., Ruyle, A. M., Sloan, A. M. & Wilson, D. A. Spatial and temporal distribution of odorant-evoked activity in the piriform cortex. *J. Neurosci.* **27**, 1534–1542 (2007).
33. Rebello, M. R. et al. Perception of odors linked to precise timing in the olfactory system. *PLoS Biol.* **12**, e1002021 (2014).
34. Rajan, R., Clement, J. P. & Bhalla, U. S. Rats smell in stereo. *Science* **311**, 666–670 (2006).
35. Gardiner, J. M. & Atema, J. The function of bilateral odor arrival time differences in olfactory orientation of sharks. *Curr. Biol.* **20**, 1187–1191 (2010).
36. von Bekesy, G. Olfactory analogue to directional hearing. *J. Appl. Physiol.* **19**, 369–373 (1964).
37. Bressler, S. L. Cortical coordination dynamics and the disorganization syndrome in schizophrenia. *Neuropsychopharmacology* **28**, S35–S39 (2003).
38. Carroll, C. A., Boggs, J., O'Donnell, B. F., Shekhar, A. & Hetrick, W. P. Temporal processing dysfunction in schizophrenia. *Brain Cogn.* **67**, 150–161 (2008).

39. Moberg, P. J. et al. Olfactory dysfunction in schizophrenia: a qualitative and quantitative review. *Neuropsychopharmacology* **21**, 325–340 (1999).
40. Olofsson, J. K. Time to smell: a cascade model of human olfactory perception based on response-time (RT) measurement. *Front. Psychol.* **5**, 33 (2014).
41. Holcombe, A. O. Seeing slow and seeing fast: two limits on perception. *Trends Cogn. Sci.* **13**, 216–221 (2009).
42. Recanzone, G. H. & Sutter, M. L. The biological basis of audition. *Annu. Rev. Psychol.* **59**, 119–142 (2008).
43. Olofsson, J. K., Bowman, N. E., Khatibi, K. & Gottfried, J. A. A time-based account of the perception of odor objects and valences. *Psychol. Sci.* **23**, 1224–1232 (2012).
44. Gupta, P., Albeanu, D. F. & Bhalla, U. S. Olfactory bulb coding of odors, mixtures and sniffs is a linear sum of odor time profiles. *Nat. Neurosci.* **18**, 272–281 (2015).
45. Lorig, T. S. On the similarity of odor and language perception. *Neurosci. Biobehav. Rev.* **23**, 391–398 (1999).
46. Lundstrom, J. N., Gordon, A. R., Alden, E. C., Boesveldt, S. & Albrecht, J. Methods for building an inexpensive computer-controlled olfactometer for temporally-precise experiments. *Int. J. Psychophysiol.* **78**, 179–189 (2010).
47. Porter, J. et al. Mechanisms of scent-tracking in humans. *Nat. Neurosci.* **10**, 27–29 (2007).
48. Wu, Y., Chen, K., Ye, Y., Zhang, T. & Zhou, W. Humans navigate with stereo olfaction. *Proc. Natl Acad. Sci. USA* **117**, 16065–16071 (2020).
49. Unno, T., Naitoh, Y., Sakamoto, N. & Horikawa, H. Nasal resistance measured by anterior rhinomanometry. *Rhinology* **24**, 49–55 (1986).
50. Yao, F., Ye, Y. & Zhou, W. Nasal airflow engages central olfactory processing and shapes olfactory percepts. *Proc. R. Soc. B* **287**, 20201772 (2020).
51. Scott, J. W., Sherrill, L., Jiang, J. & Zhao, K. Tuning to odor solubility and sorption pattern in olfactory epithelial responses. *J. Neurosci.* **34**, 2025–2036 (2014).
52. Schab, F. R. Odor memory: taking stock. *Psychol. Bull.* **109**, 242–251 (1991).
53. Ye, Y. et al. Decomposition of an odorant in olfactory perception and neural representation. *Nat. Hum. Behav.* **8**, 1150–1162 (2024).

Acknowledgements

We thank Y. Zhu for assistance with the PID recordings. This work was supported by STI2030-Major Projects 2021ZD0204200 (W.Z.), the Chinese Academy of Sciences Grant No. JCTD-2021-06 (W.Z.), the National Natural Science Foundation of China Grant Nos 32430043 (W.Z.) and 32200865 (Y.W.), the China Postdoctoral Science Foundation Grant No. 2022M713345 (Y.W.), and the Institute of Psychology, Chinese Academy of Sciences Grant No. E2CX6725CX (Y.W.). The funders had no role in study design, data collection and analysis, decision to publish or preparation of the manuscript.

Author contributions

W.Z. conceptualized the study. Y.W., K.C., C.X. and M.H. performed the experiments. K.Z. supervised the PID and gas chromatography-flame ionization detector (GC-FID) measurements. Y.W. and K.C. analysed the data under the supervision of W.Z. Y.W. and W.Z. wrote the original draft. Y.W., K.Z. and W.Z. revised the manuscript.

Competing interests

The authors declare no competing interests.

Additional information

Supplementary information The online version contains supplementary material available at https://doi.org/10.1038/s41562-024-01984-8.

Correspondence and requests for materials should be addressed to Wen Zhou.

Peer review information *Nature Human Behaviour* thanks Nitin Gupta, Dmitry Rinberg and the other, anonymous, reviewer(s) for their contribution to the peer review of this work. Peer reviewer reports are available.

nature portfolio

Corresponding author(s): Wen Zhou

Last updated by author(s): Aug 5, 2024

Reporting Summary

Nature Portfolio wishes to improve the reproducibility of the work that we publish. This form provides structure for consistency and transparency in reporting. For further information on Nature Portfolio policies, see our Editorial Policies and the Editorial Policy Checklist.

Statistics

For all statistical analyses, confirm that the following items are present in the figure legend, table legend, main text, or Methods section.

n/a	Confirmed
☐	☒ The exact sample size (*n*) for each experimental group/condition, given as a discrete number and unit of measurement
☐	☒ A statement on whether measurements were taken from distinct samples or whether the same sample was measured repeatedly
☐	☒ The statistical test(s) used AND whether they are one- or two-sided *Only common tests should be described solely by name; describe more complex techniques in the Methods section.*
☒	☐ A description of all covariates tested
☐	☒ A description of any assumptions or corrections, such as tests of normality and adjustment for multiple comparisons
☐	☒ A full description of the statistical parameters including central tendency (e.g. means) or other basic estimates (e.g. regression coefficient) AND variation (e.g. standard deviation) or associated estimates of uncertainty (e.g. confidence intervals)
☐	☒ For null hypothesis testing, the test statistic (e.g. *F*, *t*, *r*) with confidence intervals, effect sizes, degrees of freedom and *P* value noted *Give P values as exact values whenever suitable.*
☒	☐ For Bayesian analysis, information on the choice of priors and Markov chain Monte Carlo settings
☒	☐ For hierarchical and complex designs, identification of the appropriate level for tests and full reporting of outcomes
☐	☒ Estimates of effect sizes (e.g. Cohen's *d*, Pearson's *r*), indicating how they were calculated

Our web collection on statistics for biologists contains articles on many of the points above.

Software and code

Policy information about availability of computer code

Data collection	LabChart 8 was used to record flow rates and vapor phase odor concentrations. The in-built software of NR6 Rhinomanometer (NR6 Clinical 3.2.0.1106) was used to record nasal pressures and flow rates. No software was used for the collection of behavioral data.
Data analysis	MATLAB 2018a, SPSS (Version 26) MATLAB scripts for analyzing airflow and PID measurements are available at https://doi.org/10.57760/sciencedb.psych.00224.

For manuscripts utilizing custom algorithms or software that are central to the research but not yet described in published literature, software must be made available to editors and reviewers. We strongly encourage code deposition in a community repository (e.g. GitHub). See the Nature Portfolio guidelines for submitting code & software for further information.

Data

Policy information about availability of data

All manuscripts must include a data availability statement. This statement should provide the following information, where applicable:

- Accession codes, unique identifiers, or web links for publicly available datasets
- A description of any restrictions on data availability
- For clinical datasets or third party data, please ensure that the statement adheres to our policy

All reported data are available at https://doi.org/10.57760/sciencedb.psych.00224.

Research involving human participants, their data, or biological material

Policy information about studies with human participants or human data. See also policy information about sex, gender (identity/presentation), and sexual orientation and race, ethnicity and racism.

Reporting on sex and gender	The study examines perceptual sensitivity to chemical dynamics within a single sniff. Sex and gender were not considered in the study design. Participants self-reported their sex. 53.3% of them were female. No sex- and gender-based analyses have been performed as the study is not designed to probe sex- or gender-related differences.
Reporting on race, ethnicity, or other socially relevant groupings	We did not collect any data on race, ethnicity or other socially constructed or socially relevant groupings as such variables were not considered in the study design.
Population characteristics	See above.
Recruitment	Participants were recruited via advertisements on social media, which could have attracted individuals who were generally well-educated and interested in olfaction. Nonetheless, these factors are unlikely to impact one's subsniff temporal sensitivity to the dynamics of olfactory input, as measured in the current study, and are unrelated to our conclusion that human olfactory perception is sensitive to chemical dynamics within a single sniff.
Ethics oversight	The study was approved by the the Institutional Review Board at the Institute of Psychology, Chinese Academy of Sciences (H22015).

Note that full information on the approval of the study protocol must also be provided in the manuscript.

Field-specific reporting

Please select the one below that is the best fit for your research. If you are not sure, read the appropriate sections before making your selection.

☐ Life sciences ☒ Behavioural & social sciences ☐ Ecological, evolutionary & environmental sciences

For a reference copy of the document with all sections, see nature.com/documents/nr-reporting-summary-flat.pdf

Behavioural & social sciences study design

All studies must disclose on these points even when the disclosure is negative.

Study description	The study has two parts. First, a sniff-triggered apparatus is developed; quantitative data are presented regarding the control of odorant deliveries within a sniff and its temporal precision. Second, the apparatus is implemented in rigorous psychophysical testing of 229 participants across six experiments to assess olfactory discrimination for two odorants presented in counterbalanced reversed orders with varying stimulus onset asynchronies. Quantitative physiological and behavioral data on sniffing and olfactory perception are presented.
Research sample	A total of 388 healthy nonsmokers participated in the behavioral assessments. Among these, 189 took part in the main experiments, 109 were screened for the supplementary experiment, and 90 rated the perceptual properties (e.g., intensity, pleasantness) of the olfactory stimuli and/or were tested for their nasal pungencies (trigeminality) . Out of those in the main experiments, 119 (60 females, 23.1 ± 2.6 yrs) were assessed for olfactory discrimination between the temporal mixtures of PV→IP and IP→PV at ΔL = 30 cm in Experiment 1. Of these, 46 (25 females, 22.4 ± 2.8 yrs) showed accuracies ≥ 0.75 and were invited for follow-up Experiments 2 and 3. There were 30 participants in each of Experiments 2 and 3 (Experiment 2: 16 females, 23.0 ± 2.3 yrs; Experiment 3: 16 females, 22.2 ± 2.2 yrs); 14 took part in both follow-ups. Another 70 participants (36 females, 23.5 ± 2.3 yrs) were assessed with CTL→DMTS and DMTS→CTL at ΔL = 30 cm in Experiment 4; of those with discrimination accuracies ≥ 0.75, thirty (18 females, 23.3 ± 1.7 yrs) were further tested in Experiment 5 at ΔL = 10 cm. Out of those screened for the supplementary experiment, 44 (26 females, 22.7 ± 2.5 yrs) showed accuracies ≥ 0.75 for the temporal mixtures of PV→IP and IP→PV at ΔL = 30 cm. Forty of these participants (23 females, 22.6 ± 2.5 yrs) were further tested for the discriminations of the vapor mixtures of PV and IP in varying ratios and of the temporal mixtures of PV→IP and IP→PV at ΔL = 10 cm. All participants self-reported having a normal sense of smell and no respiratory allergy or upper respiratory infection at the time of testing. The samples in Experiments 1 and 4, as well as in the odor evaluation/lateralization tests, were generally representative of healthy young nonsmokers with a normal sense of smell. In contrast, the samples in Experiments 2, 3, and 5, along with those in the supplementary experiment, were recruited due to their superior performance in discriminating between temporal odor mixtures at ΔL = 30 cm, and thus were not representative. We note that these experiments were conducted to probe the upper limit of subsniff temporal sensitivity in human olfactory perception and to rule out confounding factors in such sensitivity.
Sampling strategy	Participants were initially sampled by convenience and then selected based on the following criteria: 18-30 years old, nonsmokers, a normal sense of smell, and no respiratory allergies or upper respiratory infections at the time of testing. Those who showed discrimination accuracies ≥ 0.75 for PV→IP and IP→PV at ΔL = 30 cm in Experiment 1 were invited to participate in Experiments 2 and 3. Those who showed discrimination accuracies ≥ 0.75 for CTL→DMTS and DMTS→CTL at ΔL = 30 cm in Experiment 4 were invited to participate in Experiment 5. Participants in the supplementary experiment also showed discrimination accuracies ≥ 0.75 for PV→IP and IP→PV at ΔL = 30 cm in the screening phase. As for sample sizes, we could not perform a formal power analysis since the one previous study we were aware of on human olfactory sensitivity to subsniff chemical dynamics showed a null result. To secure statistical power, we employed a large sample size

	of 119 in Experiment 1, which was estimated to have 90% power to detect even a relatively small effect size of Cohen's d = 0.3. Experiment 1 turned out to yield a medium to large effect size of Cohen's d = 0.71. We thus employed a slightly smaller sample size of 70 in Experiment 4, which tested the generalizability of the results obtained in Experiment 1. This sample size was estimated to have 90% power to detect a small to medium effect size of Cohen's d = 0.4. Experiment 4 again yielded a medium to large effect size of Cohen's d = 0.63. Experiments 2, 3, and 5 were conducted to probe the upper limit of subsniff temporal sensitivity in human olfactory perception and to rule out confounding factors in such sensitivity. The participants in these experiments were recruited due to their superior discrimination performances in Experiments 1 and 4. We expected the effects to be larger in size than in unscreened samples. The sample size for each of these experiments was 30, which was estimated to have 90% power to detect an effect size of Cohen's d = 0.6, and was about 2-3 times the size used in previous studies on related topics (e.g., Laing et al., 1994; Perl et al., 2020). Please refer to https://doi.org/10.17605/OSF.IO/7WTEU for the sample size rationale for the preregistered supplementary experiment.
Data collection	Flow rates were recorded using a spirometer (ADInstruments, New Zealand) or a rhinomanometer (NR6, GM Instruments, UK). Stimulus onset asynchronies (SOAs) between the two valve-gated odor channels were measured with two calibrated miniature photo-ionization detectors (Aurora Scientific, Canada). Participants were individually assessed by an experimenter in a well-ventilated room, with no one else present. The participants were blindfolded during testing (see Behavioral assessments for details) and were thus blind to experimental conditions. The experimenter was aware of the conditions due to the nature of odor presentations in this study but was blind to the study hypothesis during data collection. Verbal reports of the participants (e.g., discrimination performances, order judgments) were recorded by pen and paper.
Timing	Data collection was affected by Covid lock-downs, device malfunctions (miniPID, check valves), and the associated troubleshooting and repairs. Data were collected from July 2018 to October 2019 and intermittently from November 2020 to March 2024.
Data exclusions	7 participants were excluded from the main experiments due to apparatus malfunction.
Non-participation	No participant dropped out of the study.
Randomization	The study employed a within-subjects design. Participants were not allocated into experimental groups.

Reporting for specific materials, systems and methods

We require information from authors about some types of materials, experimental systems and methods used in many studies. Here, indicate whether each material, system or method listed is relevant to your study. If you are not sure if a list item applies to your research, read the appropriate section before selecting a response.

Materials & experimental systems

n/a	Involved in the study
☒	☐ Antibodies
☒	☐ Eukaryotic cell lines
☒	☐ Palaeontology and archaeology
☒	☐ Animals and other organisms
☒	☐ Clinical data
☒	☐ Dual use research of concern
☒	☐ Plants

Methods

n/a	Involved in the study
☒	☐ ChIP-seq
☒	☐ Flow cytometry
☒	☐ MRI-based neuroimaging